Available online at www.sciencedirect.com
SCIENCE DIRECT®
Journal of Solid State Chemistry 178 (2005) 3662–3666
JOURNAL OF SOLID STATE CHEMISTRY
www.elsevier.com/locate/jssc

Structural disorder in $Ba_{0.6}Sr_{0.4}Al_2O_4$

Koichiro Fukuda*, Tomoyuki Iwata, Takashi Orito

Department of Environmental and Materials Engineering, Nagoya Institute of Technology, Nagoya 466-8555, Japan

Received 5 August 2005; received in revised form 5 September 2005; accepted 11 September 2005
Available online 10 October 2005

Abstract

The structural disorder in $Ba_{0.6}Sr_{0.4}Al_2O_4$ (space group $P6_322$) was investigated by X-ray powder diffraction and selected-area electron diffraction (SAED). The initial structural model was determined using direct methods, and it was further modified by the combined use of Rietveld method and maximum-entropy method (MEM). MEM-based pattern fitting method was subsequently applied, resulting in the final reliability indices of $R_{wp} = 9.61\%$, $R_p = 6.96\%$, $R_B = 1.40\%$ and $S = 1.25$. The electron density distribution was satisfactorily expressed by the split-atom model in which the strontium/barium and oxygen atoms were split to occupy the lower symmetry sites. The diffuse scattering in SAED was mainly attributable to the positional disorder of oxygen atoms.

Keywords: Barium strontium aluminate; Selected-area electron diffraction; X-ray powder diffraction; Rietveld method; Maximum-entropy method; Electron density distribution

1. Introduction

Crystals of strontium aluminate ($SrAl_2O_4$) and barium aluminate ($BaAl_2O_4$) are promising host materials for long afterglow luminescence [1,2]. In the $BaAl_2O_4$–$SrAl_2O_4$ system, a series of powder specimens has been examined using a transmission electron microscope (TEM) [3]. For the crystals with $Ba/(Ba+Sr) = 0.6$, 0.8 and 0.9, the selected-area electron diffraction (SAED) patterns have demonstrated diffuse streaks along $\langle 110 \rangle^*$. In general, the diffuse scattering in reciprocal space can indicate some kind of structural disorder, which includes positional disorder of individual atoms and/or orientational disorder of rigid atomic groups [4]. The origin of the present diffuse scattering has not been elucidated so far.

Recently, Yamada et al. [5] have revealed the positional disorder of oxygen atoms in Eu-doped $SrAl_2O_4$ (space group $P6_322$). They investigated the complicated structure with X-ray powder diffraction data by the combined use of Rietveld method and maximum-entropy method (MEM) [6], and eventually MEM-based pattern fitting (MPF) method [7]. The electron density distribution (EDD) was visualized, followed by the modification of the initial model into the split-atom model. The MEM/Rietveld method is, however, insufficient to readily determine a charge density because the observed structure factors, F_o (Rietveld), are biased toward the structural model. The subsequent MPF method reduces the bias as much as possible. Thus, the MEM and MPF analyses were alternatively repeated (REMEDY cycle) until the reliability indices no longer decrease.

The $SrAl_2O_4$ crystal undergoes a phase transformation from monoclinic to hexagonal at 950 K during heating [8]. The hexagonal phase at 1073 K showed a superstructure with unit-cell parameters $\sqrt{3}A$ and C [9], where A and C correspond to the lattice parameters of hexagonal tridymite. At ambient temperature, the $BaAl_2O_4$ is hexagonal having a superstructure with unit-cell parameters $2A$ and C [10,11]. These crystals are of the stuffed tridymite derivatives, the structures of which are characterized by the orientation and linkage pattern of the $[AlO_4]$ tetrahedra.

In the present study, we have investigated the structural disorder in $Ba_{0.6}Sr_{0.4}Al_2O_4$ by SAED and MEM/Rietveld methods. The EDD was satisfactorily expressed by a split-atom model, in which the oxygen and barium/strontium atoms were split to occupy the lower symmetry sites.

*Corresponding author. Fax: +81 52 735 5289.
E-mail address: fukuda.koichiro@nitech.ac.jp (K. Fukuda).

0022-4596/$ - see front matter © 2005 Elsevier Inc. All rights reserved.
doi:10.1016/j.jssc.2005.09.015

2. Experimental

2.1. Synthesis

The present specimen of barium strontium aluminate ($Ba_{0.6}Sr_{0.4}Al_2O_4$) was prepared from stoichiometric amounts of reagent-grade chemicals $BaCO_3$, $SrCO_3$ and Al_2O_3. The mixture was pressed into pellets (12 mm diameter and 3 mm thick), heated at 1773 K for 1 h, followed by quenching in air.

2.2. Characterization

SAED patterns were obtained using TEM (JEM 2010) operated at 200 kV and equipped with a double tilting stage. X-ray powder diffraction intensities were collected at 298 K on a PANalytical X'Pert diffractometer in the Bragg–Brentano geometry using monochromatized Cu$K\alpha$ radiation (50 kV, 40 mA) and a step-scan technique with a 2θ range of 18–149.98° and a fixed counting time of 15 s/step and a step interval of 0.02°. The divergence slit of 0.5° was employed, which enabled us to collect the quantitative profile intensities in the 2θ range.

The three-dimensional EDD and crystal-structure models were visualized with a software package VENUS [12].

3. Results and discussion

3.1. Initial structural model

The SAED patterns in Fig. 1 showed distinct diffuse streaks along $\langle 110 \rangle^*$, together with sharp diffraction spots corresponding to the unit cell of A (≈ 0.52 nm) and C (≈ 0.86 nm). These diffraction features are in accord with those observed for the $(Ba_xSr_{1-x})Al_2O_4$ crystals with $x = 0.6$, 0.8 and 0.9 [3]. Because the diffuse streaks necessarily appeared perpendicular to the c-axis, the directions of the corresponding structural disorder must be parallel to (001) within the unit cell.

With powder diffraction, peak positions were determined after $K\alpha_2$ stripping on a computer program POWDERX [13], followed by the indexing procedure on a computer program TREOR90 [14]. In the latter procedure, 2θ values of 37 peak positions were used as input data. Only one hexagonal cell was found with satisfactory figures of merit $M_{20}/F_{20} = 47/40(0.01870, 27)$, $M_{30}/F_{30} = 45/37(0.01595, 0)$ and $M_{37}/F_{37} = 40/27(0.01598, 87)$ [15,16]. The derived unit-cell parameters, $a = 0.51849(2)$ nm and $c = 0.86299(8)$ nm, could index all reflections in the observed diffraction pattern. The derived unit-cell dimensions agree well with those determined by the SAED patterns.

The refined integrated intensities were examined to confirm the presence and absence of reflections. There were systematic absence $l \neq 2n$ for $000l$ reflections, implying that the possible space groups are $P6_3$, $P6_3/m$ and $P6_322$. All of the possible space groups were tested using an EXPO2004 package [17] for crystal-structure determination. A minimum reliability index R_F [18] of 7.91% was obtained with the space group $P6_322$ in a default run of the program. Structural parameters of all atoms were subsequently refined by the Rietveld method on a computer program RIETAN-2000 [19] using the profile intensity data in the 2θ range of 18–149.98°. The background intensities were fitted to a polynomial function with 10 adjustable parameters. The split pseudo-Voigt function [20] was used to fit the peak profile. Isotropic atomic displacement parameters, B, were assigned to all atoms. The refined positional and displacement parameters of atoms are given in Table 1. Reliability indices [18] were $R_{wp} = 10.98\%$, $R_p = 8.21\%$, $R_B = 4.21\%$ and $S = 1.45$. The displacement

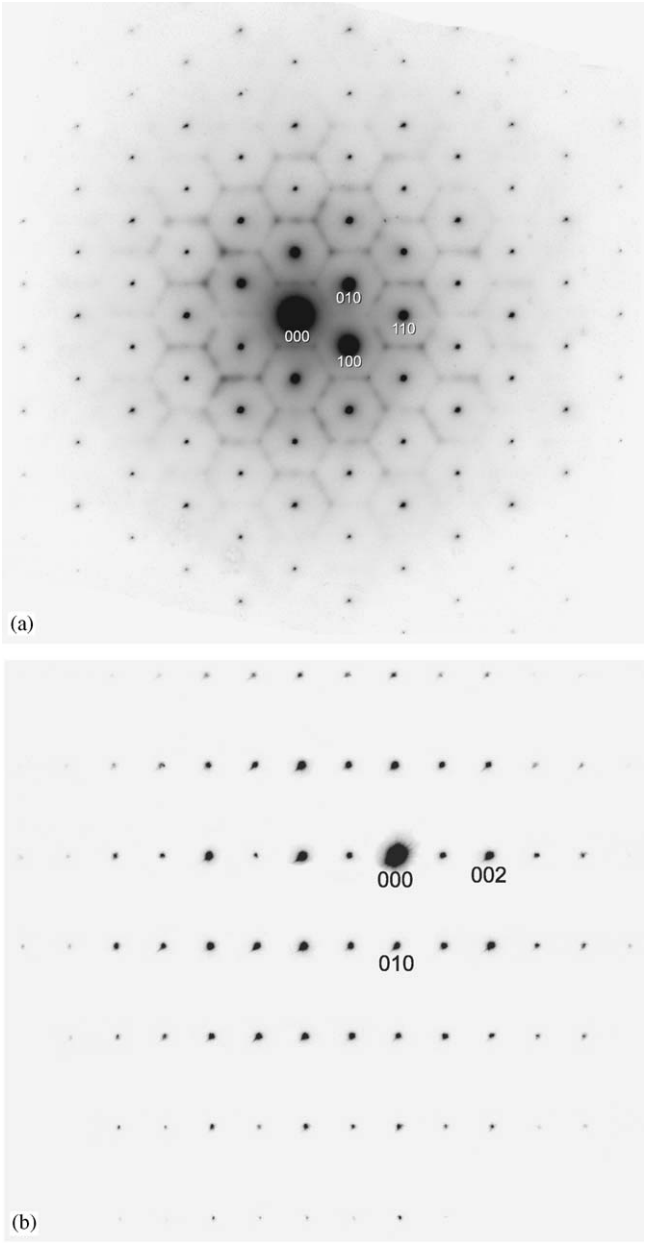

Fig. 1. Selected-area electron diffraction patterns. Incident beam nearly parallel to [001] in (a) and [100] in (b).

Table 1
Structural parameters for the initial model

Atom	Site	g	x	y	z	B (nm^2)
Ba,Sr[a]	2*b*	1	0	0	1/4	0.0120(1)
Al	4*f*	1	1/3	2/3	0.9457(2)	0.0135(4)
O1	2*d*	1	1/3	2/3	3/4	0.098(3)
O2	6*g*	1	0.3644(6)	0	0	0.0237(9)

[a]Ba/(Ba + Sr) = 0.6.

parameters of oxygen ions showed particularly large values.

Ionic radii of Al^{3+} in the fourfold coordination [$r(Al^{3+}) = 0.039$ nm and $r(O^{2-}) = 0.138$ nm] predict the interatomic distance of 0.177 nm for Al–O [21]. With monoclinic $SrAl_2O_4$, the mean Al–O bond length ($= \langle Al–O \rangle_m$) is 0.175 nm [22]. These values are in good agreement with the interatomic distance of 0.1720(1) nm for Al–O2. On the other hand, the Al–O1 distance (0.1690(1) nm) is appreciably shorter than those Al–O distances. Furthermore, the Al–O1–Al bond angle (180°) is far apart from those of the monoclinic $SrAl_2O_4$; the Al–O–Al angle ranges from 120.5° to 137.9° [22].

In order to visualize the EDD and subsequently modify the initial structural model, MEM has been applied to the present Rietveld result on a computer program PRIMA [7]. The EDD at the Ba/Sr (2*b*) site was slightly elongated along the *c*-axis (Fig. 2(a)). The EDD at the O1 (2*d*) and O2 (6*g*) sites showed broadening (Fig. 1(a)), which would correspond to the large displacement parameters of the oxygen atoms. With Al site, the EDD was in accord with the atomic positions of the initial model. The two-dimensional map (Fig. 2(b)) demonstrated that the oxygen atoms at 2*d* site are split to occupy the three sites around the threefold axis. Accordingly, the initial model was, in the subsequent refinement process, modified to a split-atom model, the site symmetry in which it decreased from 2*b* to 4*e* for Ba/Sr, 2*d* to 6*h* for O1 and 6*g* to 12*i* for O2.

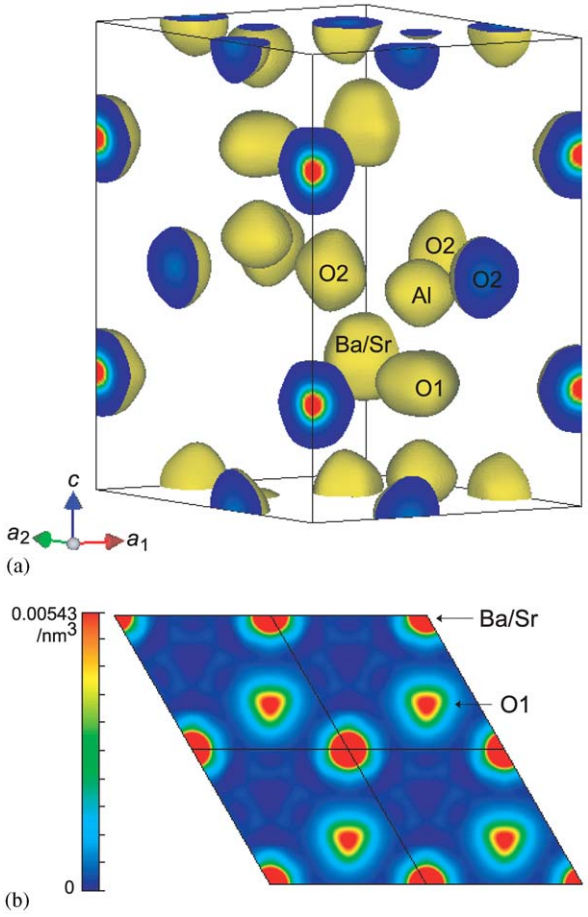

Fig. 2. Electron density distribution determined by MEM/Rietveld method with the initial model. (a) Isosurface for an equidensity level of 0.0016 nm^{-3}; (b) two-dimensional map on the (004) section.

3.2. Split-atom model

In the split-atom model, the reliability indices ($R_{wp} = 9.72\%$, $R_p = 7.05\%$, $R_B = 2.29\%$ and $S = 1.28$) as well as the B values of O1 and O2 significantly decreased as compared with those of the initial model. The crystal data are given in Table 2, and positional and thermal parameters of atoms are given in Table 3. The MPF method was subsequently applied, so as to extract structural details and consequently improve the EDD. After one REMEDY cycle, R_{wp}, R_p, R_B and S decreased to 9.61%, 6.96%, 1.40% and 1.27, respectively (Fig. 3). The EDD at the Ba/Sr (4*e*) site was slightly elongated along the *c*-axis (Fig. 4(a)). The O2 (12*i*) site showed elongated EDD nearly along the *c*-axis. The EDD on (004) at the O1 (6*h*) site clearly demonstrated the three sharp maximum around the threefold axis (Fig. 4(b)). The positional disorder of the oxygen atoms as described above is consistent with that as determined in Eu-doped $SrAl_2O_4$ [5].

In the [AlO_4] tetrahedra (Fig. 5), the Al–O1 bond length (Table 4) is in good agreement with those of monoclinic $SrAl_2O_4$; $\langle Al–O \rangle_m = 0.175$ nm [22]. On the other hand, there are two distinct interatomic distances for Al–O2. Although the mean bond length (0.174 nm) agrees well with $\langle Al–O \rangle_m$, each of the bond lengths is far apart from it (Table 4). This implies that the aluminium atoms are also displaced from their average position of the 4*f* site to the lower symmetry (probably 12*j*) site. Because the EDD of the aluminium atoms is almost spherical (Fig. 4(a)), the displacement magnitude would be too small to refine the

positional parameter. Accordingly, the whole [AlO_4] tetrahedra would be orientationally disordered around the threefold axis. The positional disorder of O1 atoms, the displacement directions of which are parallel to (001), would mainly cause the diffuse scattering as observed in the SAED pattern (Fig. 1(a)).

4. Conclusion

The structural disorder in $Ba_{0.6}Sr_{0.4}Al_2O_4$ at 298 K was investigated using SAED, MEM/Rietveld and MPF methods. The structure was hexagonal (space group $P6_322$, $Z = 2$) with $a = 0.51879(1)$ nm, $c = 0.86385(1)$ nm and $V = 0.201352(6)$ nm^3. The EDD was satisfactorily expressed by the split-atom model, the site symmetry in which was 4*e* for Ba/Sr, 6*h* for O1 and 12*i* for O2. The EDD for oxygen atoms of the 6*h* site demonstrated the three sharp maximum around the threefold axis, and that

Table 2
Crystal data of barium strontium aluminate

Chemical composition	$Ba_{0.6}Sr_{0.4}Al_2O_4$
Space group	$P6_322$
a (nm)	0.51879(1)
c (nm)	0.86385(1)
V (nm^3)	0.201352(6)
Z	2
D_x (Mg m^{-3})	3.88

Table 3
Structural parameters for the split-atom model

Atom	Site	g	x	y	z	B (nm^2)
Ba,Sr[a]	4*e*	1/2	0	0	0.2616(3)	0.0094(2)
Al	4*f*	1	1/3	2/3	0.9452(1)	0.0123(3)
O1	6*h*	1/3	0.388(1)	2*x*	3/4	0.024(2)
O2	12*i*	1/2	0.366(1)	0.007(2)	0.0314(5)	0.0065(9)

[a]Ba/(Ba + Sr) = 0.6

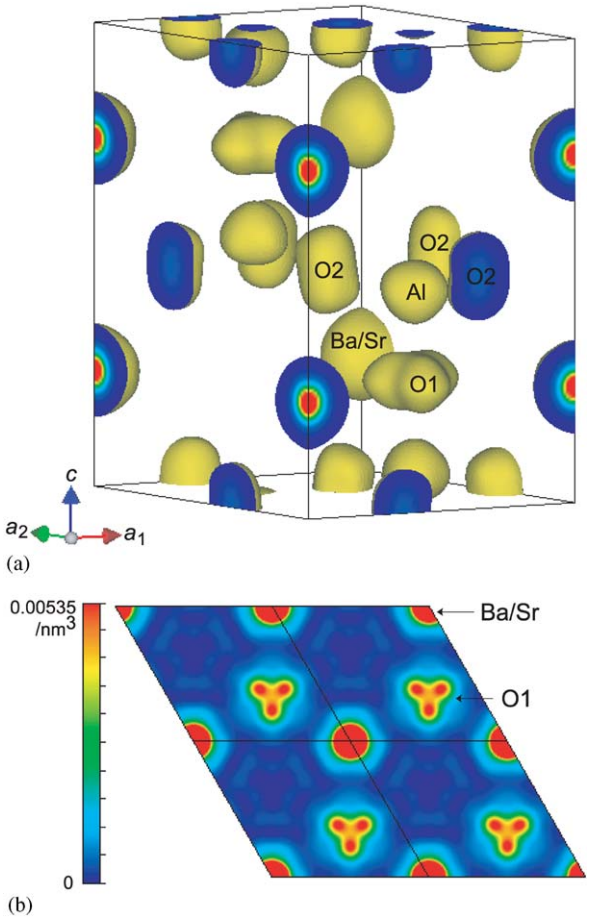

Fig. 4. Electron density distribution determined by MPF method with the split-atom model. (a) Isosurface for an equidensity level of 0.0016 nm^{-3}; (b) two-dimensional map on the (004) section.

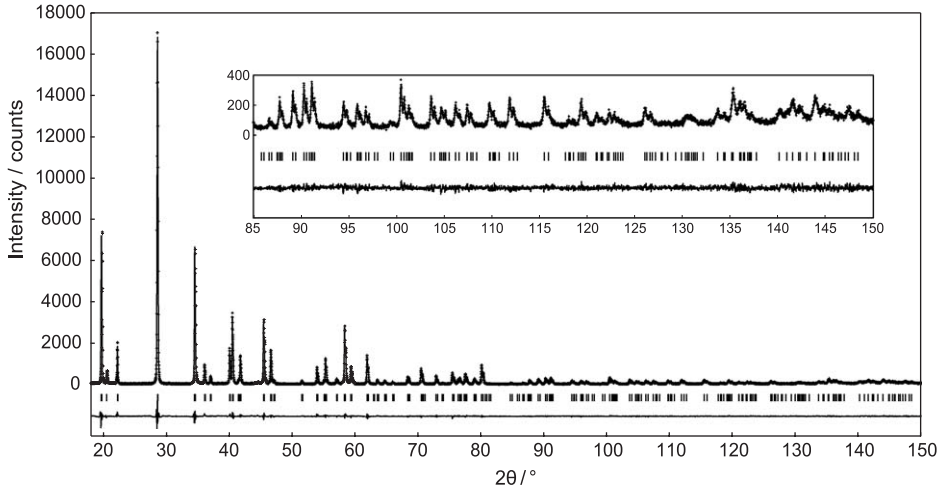

Fig. 3. Comparison between observed (+ marks) and calculated (upper solid line) patterns obtained by the final MPF structure refinement. The difference curve is shown in the lower part of the figure. Vertical marks indicate the positions of possible Bragg reflections.

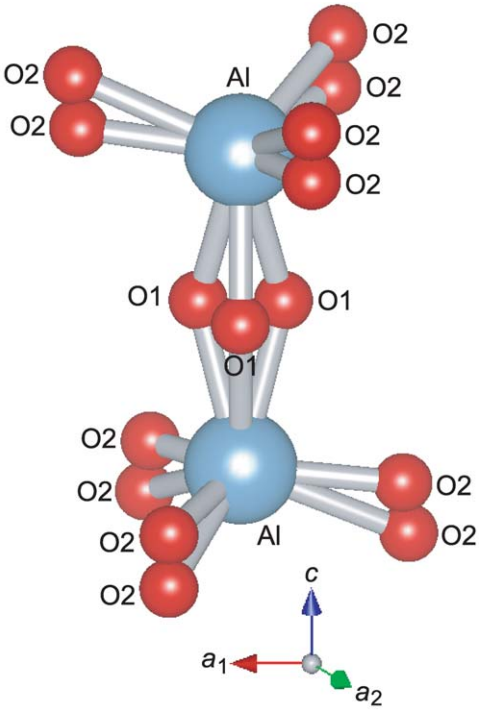

Fig. 5. Coordination sphere of oxygen atoms around the Al atoms with the split-atom model.

Table 4
Bond lengths (nm) and bond angles (°) for the split-atom model

Al–O1	0.1757(3)
Al–O2	0.1642(8) or 0.1846(7) (the mean = 0.174)
Al–O1[a]–Al[b]	147.3(5)
Al–O2[c]–Al[d]	128.4(2)

Symmetry transformations used to generate equivalent atoms.
(a) $1-y$, $1+x-y$, z; (b) $1-y$, $1-x$, $3/2-z$; (c) $1-x$, $1-x+y$, $1-z$; (d) y, x, $2-z$.

of the 12*i* site showed elongation nearly along the *c*-axis. The positional disorder of oxygen atoms would mainly cause the diffuse scattering in the reciprocal space.

References

[1] H. Takasaki, S. Tanabe, T. Hanada, J. Ceram. Soc. Jpn. 104 (1996) 322–326.
[2] Y. Lin, Z. Zhang, Z. Tang, J. Zhang, Z. Zheng, X. Lu, Mater. Chem. Phys. 70 (2001) 156–159.
[3] U. Rodehorst, M.A. Carpenter, S. Marion, C.M.B. Henderson, Miner. Mag. 67 (2003) 989–1013.
[4] G. Van Tendeloo, S. Amelinckx, Phase Transit 67 (1998) 101–135.
[5] H. Yamada, W.S. Shi, C.N. Xu, J. Appl. Crystallogr. 37 (2004) 698–702.
[6] M. Takata, E. Nishibori, M. Sakata, Z. Kristallogr. 216 (2001) 71–86.
[7] F. Izumi, S. Kumazawa, T. Ikeda, W.-Z. Hu, A. Yamamoto, K. Oikawa, Mater. Sci. Forum 378–381 (2001) 59–64.
[8] C.M.B. Henderson, D. Taylor, Miner. Mag. 45 (1982) 111–127.
[9] K. Fukuda, K. Fukushima, J. Solid State Chem. 178 (2005) 2709–2714.
[10] W. Hoerkner, H. Mueller-Buschbaum, Z. Allg. Chem. 451 (1979) 40–44.
[11] S.-Y. Huang, R. Von Der Muhll, J. Ravez, J.P. Chaminade, P. Hagenmuller, M. Couzi, J. Solid State Chem. 109 (1994) 97–105.
[12] F. Izumi, R.A. Dilanian, in: Recent Research Developments in Physics, Part II, vol. 3, Transworld Research Network, Trivandrum, India, 2002, pp. 699–726.
[13] C. Dong, J. Appl. Crystallogr. 32 (1999) 838.
[14] P.E. Werner, L. Eriksson, M. Westdahl, J. Appl. Crystallogr. 18 (1985) 367–370.
[15] P.M. de Wolff, J. Appl. Crystallogr. 1 (1968) 108–113.
[16] G.S. Smith, R.L. Snyder, J. Appl. Crystallogr. 12 (1979) 60–65.
[17] A. Altomare, M.C. Burla, M. Camalli, B. Carrozzini, G.L. Cascarano, C. Giacovazzo, A. Guagliardi, A.G.G. Moliterni, G. Polidori, R. Rizzi, J. Appl. Crystallogr. 32 (1999) 339–340.
[18] R.A. Young, in: R.A. Young (Ed.), The Rietveld Method, Oxford University Press, Oxford, UK, 1993, pp. 1–38.
[19] F. Izumi, T. Ikeda, Mater. Sci. Forum 321–324 (2000) 198–203.
[20] H. Toraya, J. Appl. Crystallogr. 23 (1990) 485–491.
[21] R.D. Shannon, Acta Crystallogr. A 32 (1976) 751–767.
[22] A.R. Schulze, H. Mueller-Buschbaum, Zeit. Anorg. Allg. Chem. 475 (1981) 205–210.